

SHARPENING OF METAL SHEETS DURING ELECTROCHEMICAL POLISHING. THEORY AND EXPERIMENTS

Petr Novák* and Ivo ROUŠAR

*Department of Inorganic Technology,
Prague Institute of Chemical Technology, 166 28 Prague 6*

Received March 30th, 1983

The electrochemical polishing with simultaneous shape changes of anodes was studied. A theory was derived based on the knowledge of basic electrochemical parameters and the solution of the Laplace equation. To this purpose, the finite element method and the finite difference method with a double transformation of the inter-electrode region were employed. Only the former method proved well and can therefore be recommended for different geometries.

The problem dealt with in the present work is analogous to electrochemical machining¹⁻⁴. The finite element method was used in the calculations, since of the known methods of solution of the Laplace equation it is most advantageous for our case⁵⁻⁷. For comparison, the calculations were done by the finite difference method with a double transformation of the interelectrode space⁴ to a rectangle. The sharpening of the edges of thin metal sheets occurs in electrochemical polishing of objects from stainless steel and is made use of in sharpening surgical tools; the electrolytes are the same as those used in electrochemical polishing.

The aim of the present work was to derive a theory of the sharpening process and to compare the calculated shape of the anode with that found experimentally. In addition, it was of interest to compare different calculation methods as to their suitability.

THEORETICAL

During electrochemical polishing of metals with direct current, the shape of the cathode is constant, whereas the anode dissolves to some extent and its shape changes. A model system (Fig. 1) consists of a thin plate anode of stainless steel with two parallel copper plate cathodes on either side embedded in an insulating material to form a plane surface. The electrode system is immersed in an aqueous solution of 20 wt.% H_2SO_4 and 60 wt.% H_3PO_4 tempered at 70°C. The gradual changes of the anode shape with time can be simulated by the following sequence of calculations.

* Present address: The J. Heyrovský Institute of Physical Chemistry and Electrochemistry, Czechoslovak Academy of Sciences, 102 00 Prague 10.

1) Calculation of the potential distribution between the cathode and the anode. 2) Calculation of the local current density at the anode. 3) For a chosen time step $\Delta\tau$, the loss of the metal due to anodic dissolution is calculated from the law of Faraday. Since oxygen evolution proceeds in addition to the metal dissolution, the corresponding current efficiency is taken into account. The loss of the anode metal is used to calculate changes in the coordinates of the points at the surface, $\gamma(x, y, z)$, which are shifted in the direction normal to the surface. Thus, a description of the new anode surface is obtained, and this the more accurately the smaller the time step $\Delta\tau$. 4) The new shape of the anode surface is approximately described by a finite set of points (x_i, y_i, z_i) , $i = 1, 2, \dots, N$. 5) Return to step 1). Calculations according to this algorithm were done by two methods: a) The finite element method⁸⁻¹⁰ was used to calculate the potential distribution in the interelectrode space in the original system of x, y -coordinates. b) The finite difference method^{3,4}. If the grid points were fixed, we should have to examine their location at the boundary after every change of the anode shape and calculate their distances from the neighbouring grid points. The method of calculation of potentials at the boundary would be very complicated, not to speak about programming, and therefore we used a double transformation of the interelectrode space enabling us to preserve the coordinates of all points during the whole calculation. Therefore, the form of the boundary conditions for the potentials need not be changed either.

For the model system in Fig. 1, considering the central electrode region, *i.e.* small values of z , we may assume that the system properties are constant in a certain region along the z axis (Fig. 2). Hence, the potential in this region is rather accurately de-

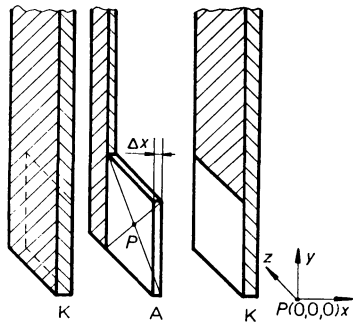


FIG. 1

Scheme of model system with coordinate axes. A stainless anode, K copper cathode. Shaded areas are covered with an insulating layer. $P(0,0,0)$ origin of coordinates, Δx anode thickness

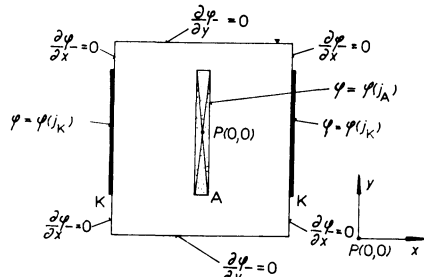


FIG. 2

Cross section through model system in the plane $z = 0$ and boundary conditions. A anode, K cathode, $P(0,0)$ origin of coordinates

scribed by the Laplace equation in two dimensions

$$\frac{\partial^2 \varphi}{\partial x^2} + \frac{\partial^2 \varphi}{\partial y^2} = 0. \quad (1)$$

Since the boundaries of the system are electrically insulated, the boundary conditions on them are $\partial\varphi/\partial x = 0$, $\partial\varphi/\partial y = 0$ (except for the electrodes). Since the system is symmetrical with respect to the plane $x = 0$, it is sufficient to solve Eq. (1) for one half of the system, e.g. for $x \geq 0$. Thus, a new boundary is formed (Fig. 3, line 1-5 and 4-8) on which the condition of symmetry $(\partial\varphi/\partial x)_{x=0} = 0$ applies, where φ denotes any property of the system.

In solving Eq. (1) in the space mentioned (Fig. 3) by the finite element method⁸⁻¹⁰, we insert grid points in it to form triangular elements in which an approximate solution will be calculated. We use the method of weighted residues: Eq. (1) is multiplied by a weight function $w(x, y)$ and integrated over the whole region Ω considered. Thus,

$$\int_{\Omega} w \left(\frac{\partial^2 \varphi}{\partial x^2} + \frac{\partial^2 \varphi}{\partial y^2} \right) d\Omega = 0. \quad (2)$$

By using Green's theorem¹¹ and the boundary conditions, Eq. (2) gives

$$\int_{\Omega} \left(\frac{\partial \varphi}{\partial x} \frac{\partial w}{\partial x} + \frac{\partial \varphi}{\partial y} \frac{\partial w}{\partial y} \right) d\Omega = 0. \quad (3)$$

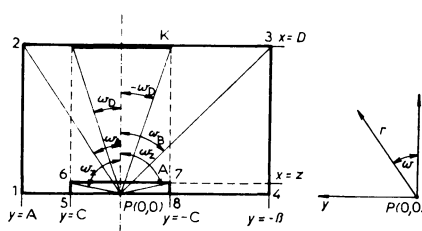
(The integral over the boundaries of the system is equal to zero.)

At this point, we introduce M base functions $F_j(x, y)$ (M is the total number of grid points) and assume that the solution at any grid point K can be approximated as

$$\varphi_K = \sum_{j=1}^M u_j F_j, \quad (4)$$

FIG. 3

Dimensions, polar angles, and coordinate axes in the interelectrode space. Cross section in the plane $z = 0$ (Fig. 1) rotated by 90° with respect to Fig. 2. Lower edge of anode corresponds to $y = -C$, upper edge to $y = C$. A anode, K cathode



where u_j denotes unknown coefficients. The weight function w_K at the grid point K is assumed to be of the form

$$w_K = F_K . \quad (5)$$

The base functions $F_j(x, y)$ are chosen so that at the grid point K we have $F_j = 0$ for $j \neq K$ and $F_K = 1$ (i.e. $F_j = \delta_{jk}$, where δ_{jk} is Kronecker's delta). Hence, at the grid points we have $u_K = \varphi_K$. Further, the base functions are defined so that in the elements only those functions are different from zero which attain the value of 1 in the apex of the element. Other base functions are in the elements identically equal to zero. For the solution of Eq. (3), it is simplest to choose the nonzero F_j functions in the elements as polynomials of the first degree.

By introducing Eqs (4) and (5) into Eq. (3), we obtain an equation for the unknown coefficients u_j (which are under the given assumptions numerically equal to the potentials at the grid points)

$$u_j \int_{\Omega} \left(\frac{\partial F_j}{\partial x} \frac{\partial F_K}{\partial x} + \frac{\partial F_j}{\partial y} \frac{\partial F_K}{\partial y} \right) d\Omega = 0 . \quad (6)$$

A local matrix is obtained for the grid points of the element considered. By combining the local matrices for the whole region Ω , we obtain a system of M linear equations, the solution of which gives an approximation of the potential distribution in the interelectrode space in the form (4).

The boundary conditions involving the electrode polarization, i.e. $\varphi_{A,K} = \varphi(j_{A,K})$, are used as follows. The potentials on the electrode surface are estimated, the Laplace equation (3) is solved, and from its solution the current density j in each point is calculated as

$$j = -\kappa_E (\text{grad } \varphi)_n , \quad (7)$$

where κ_E denotes the electrolyte conductivity. The potential gradient is calculated from the differentiated equation (4).

The electrode potential corresponding to a given current density j is calculated from the Tafel equation

$$\varphi_A = U - E_{r,A} - a_A - b_A \ln j , \quad (8)$$

$$\varphi_K = E_{r,K} + a_K + b_K \ln |j| . \quad (9)$$

Here, U denotes the terminal voltage, E_r the equilibrium potential, and a and b constants with subscripts A, K referring to anode and cathode.

In further calculations, we take a proportional part from the calculated electrode potential

$$\varphi_{A,K}^{s+1} = \varphi_{A,K}^N C^* + \varphi_{A,K}^s (1 - C^*) . \quad (10)$$

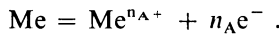
Superscript N refers to the newly calculated potential value, s denotes the iteration sequence, and C^* is an empirical constant, which may be modified during the calculations. In our case, its values were in the interval from 0.01 to 0.5.

The potential values $\varphi_{A,K}^{s+1}$ are now used as new boundary conditions for the solution of the Laplace equation. The iteration is repeated until the potentials at the electrode surfaces converge with an error less than 10^{-4} V.

At this point, the change of the anode shape is calculated. We assume that the current density at the electrode surface is constant during a short time interval $\Delta\tau$, so that the shift of the anode surface along the normal, Δn (cm), can be calculated as

$$\Delta n = \frac{M_A j_n \Delta\tau}{n_A F \varrho_A} p_1 , \quad (11)$$

where p_1 is the current efficiency in the anodic metal dissolution



Since the finite element method using polynomials of the first degree gives a constant current density on the whole side of a triangular element (compare Eqs (4) and (7)), the change of the anode shape is calculated so that the side of the element lying at the anode is shifted by Δn along the normal to the anode surface. New grid points at the electrode surface are then obtained as intersections of the shifted sides of the triangles lying next to one another.

When the values of $\Delta\tau$ and thus the shape changes are sufficiently small, the errors in the calculations are also small. The above calculation of the new anode shape corresponds to the Euler integration method.

With the method of finite differences using a double transformation, the procedure was already described⁴. The Laplace equation (1) is transformed into polar coordinates r and ω

$$\frac{\partial^2 \varphi}{\partial r^2} + \frac{1}{r} \frac{\partial \varphi}{\partial r} + \frac{1}{r^2} \frac{\partial^2 \varphi}{\partial \omega^2} = 0 . \quad (12)$$

A part of the border of the interelectrode space (1-2-3-4 in Fig. 3) is described by a curve $r = \beta(\omega)$, and another part (5-6-7-8 in Fig. 3) by a curve $r = \alpha(\omega)$.

New coordinates ξ and η are then defined as

$$\xi = \omega, \quad \eta = \frac{r(\omega) - \alpha(\omega)}{\beta(\omega) - \alpha(\omega)}, \quad (13), (14)$$

where $\xi \in \langle -\frac{1}{2}\pi, +\frac{1}{2}\pi \rangle$ and $\eta \in \langle 0, 1 \rangle$. The potential φ can then be expressed as function of the new variables $\psi(\xi, \eta)$, so that $\psi[\xi(r, \omega), \eta(r, \omega)] = \varphi(r, \omega)$. The interelectrode space is transformed to a rectangle (in the coordinates ξ and η) and the Laplace equation (12) takes the form

$$\frac{1}{r^2} \frac{\partial^2 \psi}{\partial \xi^2} + \left[\left(\frac{\partial \eta}{\partial r} \right)^2 + \frac{1}{r^2} \left(\frac{\partial \eta}{\partial \omega} \right)^2 \right] \frac{\partial^2 \psi}{\partial \eta^2} + \frac{2}{r^2} \frac{\partial \eta}{\partial \omega} \frac{\partial^2 \psi}{\partial \xi \partial \eta} + \left(\frac{1}{r} \frac{\partial \eta}{\partial r} + \frac{1}{r^2} \frac{\partial^2 \eta}{\partial \omega^2} \right) \frac{\partial \psi}{\partial \eta} = 0. \quad (15)$$

Here, r is expressed from Eq. (14). The transformed equation (15) is solved by the overrelaxation method using finite differences. A two-dimensional nonequidistant grid is placed in the interelectrode space and the derivatives are approximated by finite-difference formulae^{3,4} with an error of $O(h^2)$. Asymmetrical difference formulae are used in calculating the current density at the boundaries.

Iterative calculation of the potential values at a grid point (i, j) is carried out by the successive overrelaxation method using the general relation

$$\psi_{i,j}^{s+1} = \psi_{i,j}^s + r_{i,j} R_{i,j}^s p^*. \quad (16)$$

Superscript s or $s + 1$ denotes the order number of the iteration. The residues $R_{i,j}^s$ are calculated by introducing the s -th potential values into the left-hand side of Eq. (15) where the derivatives are expressed by the difference formulae.

Convergence of potentials ψ^s was achieved by the following choice of the relaxation factor $r_{i,j}$

$$r_{i,j}^{-1} = \frac{2}{h^2} |G_1(\xi, \eta)| + \frac{2}{g^2} |G_2(\xi, \eta)| + \frac{1}{g} |G_3(\xi, \eta)| + \frac{1}{gh} |G_4(\xi, \eta)|, \quad (17)$$

where $h = \text{Min} [(\xi_{i+1} - \xi_i), (\xi_i - \xi_{i-1})]$ and $g = \text{Min} [(\eta_{j+1} - \eta_j), (\eta_j - \eta_{j-1})]$. The meaning of the functions G_1 to G_4 is obvious from the comparison of Eq. (15) with the following Eq. (18).

$$\frac{\partial^2 \psi}{\partial \xi^2} G_1(\xi, \eta) + \frac{\partial^2 \psi}{\partial \eta^2} G_2(\xi, \eta) + \frac{\partial \psi}{\partial \eta} G_3(\xi, \eta) + \frac{\partial^2 \psi}{\partial \xi \partial \eta} G_4(\xi, \eta) = 0. \quad (18)$$

The coefficient p^* in Eq. (16) is an empirical constant which ensures and accelerates the convergence. It is preferable to use its maximum value at which the system still converges at a given instant. In our case, p^* was in the interval $\langle 0.8, 1.5 \rangle$.

The method of calculating the shape changes of the anode is analogous to the case of the finite element method. The current density values are calculated from Eq. (7) in combination with (13) and (14). The finite difference method, in contrast to the other method, gives the current density values only at the grid points at the electrode surface. The shift of the points Δn (according to Eq. (11)) is used to calculate the new coordinates of the grid points (x_i^N, y_i^N) at the electrode surface. These are recalculated to polar coordinates (ω_i^N, α_i^N) , which in turn give by quadratic interpolation the polar coordinates of points on the new surface corresponding to the original grid points given beforehand.

In total 100 grid points were used in the finite element method. The form of the coordinate grid with the triangular elements is shown in Fig. 5 (this was chosen according to ref.¹²). The program system MKP-F was used¹² and the subroutines were written in FORTRAN. The calculations were carried out on an ICL 4-72 computer; the calculation of one step of the time change of the anode took about 10 s of computer time.

EXPERIMENTAL

The model system shown in Fig. 1 was used also in the experiments. The anode was made of stainless steel Cr 18 Ni 10 and its chemical composition (in wt.%) was: C 0.085, Si 0.66, S 0.013, W 0.01, Cu 0.07, Mn 1.3, Cr 17.69, Ni 10.39, Mo 0.4, and Ti 0.56. Both cathodes were made

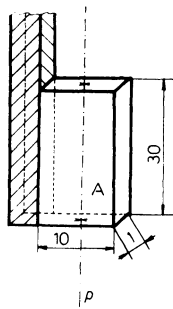


FIG. 4a

Dimensions of anode (A) and cathode (K) in mm. Shaded areas are covered with an insulating layer. Measurement by Trioptic apparatus was carried out along line p

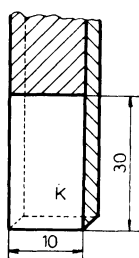
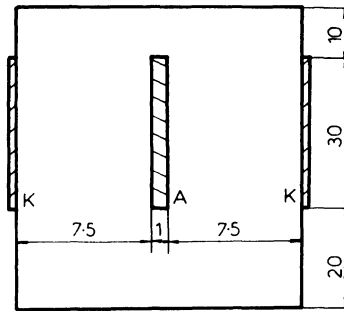


FIG. 4b

Cell dimensions in mm in cross section



of copper. The electrode dimensions (in mm) prior to polishing are given in Fig. 4. The electrode system was immersed in a laboratory vessel with an electrolyte containing sulphuric acid, phosphoric acid, and water in the mass ratio 1 : 3 : 1; its conductivity was $29.02 \Omega^{-1} \text{ m}^{-1}$ and its temperature was kept at 70°C. The current density was 0.5 A/cm^2 referred to the cathode surface area. The lower electrode edges were 20 mm above the cell bottom, the electrolyte level was 10 mm above the upper electrode edges, and the distance between the anode and cathode surfaces was 7.5 mm.

The shape change of the anode was determined by measurement of its profile on a Trioptic apparatus (SIP, Switzerland). The thickness of the sample was measured on line *p* (Fig. 4a) at points 0.5 mm apart.

Four experiments with the time of dissolution 20, 40, 80, and 120 min were done and the measured anode profiles are shown in Fig. 6. The values of the variables were as follows. Lengths (Fig. 3, 4a and 4b) $A = 25 \text{ mm}$, $B = 35 \text{ mm}$, $C = 15 \text{ mm}$, $D = 8 \text{ mm}$, $Z = 0.5 \text{ mm}$. The total current was maintained at 1.5 A. The current efficiency p_1 was determined as 38% (referred to the metal dissolution). For the given steel, $M_A/n_A = 25.31$. The constants in Eqs (8) and (9) were $E_{rA} = 1.0 \text{ V}$, $E_{rK} = -0.4 \text{ V}$, $a_A = 1.503 \text{ V}$, $b_A = 0.218 \text{ V}$, $a_K = 0.39 \text{ V}$, $b_K = 0.06 \text{ V}$. The density of the anode metal $\rho_A = 7.83 \text{ g/cm}^3$. The changes in the anode shape were calculated at time steps $\Delta\tau = 60 \text{ s}$.

DISCUSSION

The anode profiles after 20, 40, 80, and 120 min calculated by the finite element method are shown in Fig. 6 together with experimental points. It is seen that the

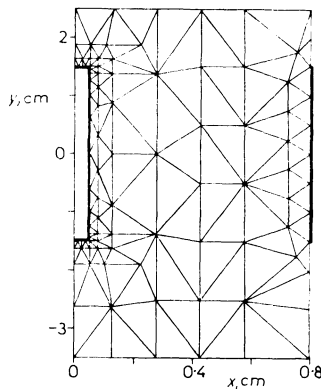


FIG. 5

Position of grid points in the finite element method at time $\tau = 0$

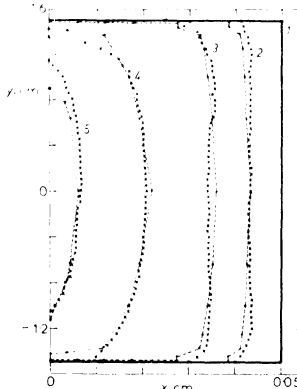


FIG. 6

Anode profiles at different times of polishing.
 1 $\tau = 0$; 2 20 min; 3 40 min; 4 80 min;
 5 120 min. Crosses denote experimental points, curves were calculated by the finite element method

agreement between theory and experiments is good, the maximum difference being about 5% of the thickness of the original sample along the x axis. For $\tau = 120$ min, the difference between theory and experiment is about 10% of the sample length in the y direction. The differences are due to calculation errors on one hand (the finite element method gives results the error of which is of the order of percent) and to a scatter of experimental results for four different dissolution times (Fig. 6) amounting to a few percent on the other hand. Another source of errors is the assumption of constant efficiency, which in reality changes to some extent with changing current density. This effect is most important at the edges of the anode, where the local current density is most different from the average.

In the finite-difference overrelaxation method, a 31×15 coordinate grid was used and all parameters were based on experimental data. However, the anode shape calculated did not correspond to reality; it showed three waves whose amplitude was after 80 min more than twice as large as the sample thickness. Thus, the calculations were useless. The reason for the failure consists in the use of the double transformation. In the finite-difference method, an approximately equidistant coordinate grid must be used. The back transformation into Cartesian coordinates results in concentrating the grid points at the electrode center. At the edges, where the process of sharpening takes place, no more than two grid points are located, which of course does not ensure the numerical stability of the calculation.

It can be concluded that the finite element method is preferable for the theory of electrochemical polishing with a complicated form of electrodes and interelectrode space. The accuracy of the calculated electrode dimensions is 5–10%, which is sufficient in practice. The finite difference method with double transformation of the interelectrode space fails in such cases.

The authors are indebted to Dr R. Žitný, Technical university, Prague, for making available the MKP-F program system, by which the finite element method programming was facilitated.

LIST OF SYMBOLS

a, b	constants of Tafel equation (V)
A, B, C	system dimensions (m)
C^*	constant
D	system dimension (m)
E_r	equilibrium potential (V)
F	Faraday's constant (96 487 C/mol)
F_i	base functions
g	grid step along η axis
G_1-G_4	functions in Eq. (18)
h	grid step along ξ axis
j	current density (A/m^2)
M_A	molar mass of anode metal (kg/mol)

n_A	number of transferred electrons in anodic dissolution
Δn	shift of anode surface along normal (m)
p_I	current efficiency in metal dissolution
p^*	multiplicative constant
r	radius vector (m)
$r_{i,j}$	relaxation factor
$R_{i,j}$	residue
u_j	multiplicative coefficient
U	terminal voltage of electrolyser (V)
w	weight function
x, y, z	Cartesian coordinates (m)
Δx	anode thickness (m)
Z	system dimension (m)
α, β	curves corresponding to system boundaries (m)
κ_E	electrolyte conductivity ($\Omega^{-1} m^{-1}$)
η	transformed r coordinate
ϱ_A	density of anode metal (kg/m ³)
ξ	transformed ω coordinate
τ	time (s)
φ	potential in Cartesian or polar coordinates (V)
ψ	potential in ξ and η coordinates (V)
Ω	region of solution
ω	polar angle

Subscripts: A anode, i, j, K summation index, K cathode, n normal component. *Superscripts:* N new value in iteration, s order number of iteration.

REFERENCES

1. Alkire R., Bergh T., Sani R. L.: J. Electrochem. Soc. 125, 1981 (1978).
2. Landolt D., Sautebin R.: J. Electrochem. Soc. 129, 946 (1982).
3. Novák P., Roušar I., Kimla A., Cežner V., Mejta V.: This Journal 45, 1867 (1980).
4. Novák P., Roušar I., Kimla A., Mejta V., Cežner V.: This Journal 46, 2949 (1981).
5. Prentice G. A., Tobias C. W.: J. Electrochem. Soc. 129, 72 (1982).
6. Prentice G. A., Tobias C. W.: J. Electrochem. Soc. 129, 78 (1982).
7. Riggs J. B., Muller R. H., Tobias C. W.: Electrochim. Acta 26, 961 (1981).
8. Zienkiewicz O. C.: *The Finite Element Method in Engineering Science*. Mc Graw-Hill, London 1971.
9. Chung T. J.: *Finite Element Analysis in Fluid Dynamics*. Mc Graw-Hill, London 1978.
10. Gallagher R. H.: *Finite Element in Fluids*, Vol. I, II. Pergamon Press, London 1973.
11. Rektorys K.: *Přehled užití matematiky*, p. 524. Published by SNTL, Prague 1968.
12. Žitný R.: *MKP-F — Metoda konečných prvků pro jedno- a dvoudimenzionální problémy*. Czech Technical University, Prague 1980.

Translated by K. Micka.